



1 Source-resolved atmospheric metal emissions, concentrations, and 2 their deposition fluxes into the East Asian Seas

3 Shenglan Jiang¹, Yan Zhang^{1,2,3*}, Guangyuan Yu¹, Zimin Han¹, Junri Zhao¹, Tianle Zhang⁴, Mei Zheng⁴

4 ¹Shanghai Key Laboratory of Atmospheric Particle Pollution and Prevention (LAP3), National Observations and Research
5 Station for Wetland Ecosystems of the Yangtze Estuary, Department of Environmental Science and Engineering, Fudan
6 University, Shanghai 200438, China

7 ²Shanghai Institute of Eco Chongming (SIEC), Shanghai 200062, China

8 ³MOE laboratory for National Development and Intelligent Governance, Shanghai institute for energy and carbon neutrality
9 strategy, IRDR ICoE on Risk Interconnectivity and Governance on Weather/Climate Extremes Impact and Public Health,
10 Fudan University, China, Fudan University, Shanghai 200433, China

11 ⁴SKL-ESPC and SEPKL-AERM, College of Environmental Sciences and Engineering, and Centre for Environment and Health,
12 Peking University, Beijing 100871, China

13 *Correspondence to:* Yan Zhang (yan_zhang@fudan.edu.cn)

14 **Abstract.** Atmospheric deposition is an important source of marine metallic elements, which have a non-negligible impact on
15 marine ecology. Atmospheric trace metals come from different sources, undergo their respective transport processes, and are
16 deposited into seas finally. This study aims to provide gridded data on sea-wide concentrations, deposition fluxes, and soluble
17 deposition fluxes with detailed source categories of metals by the modified Community Multiscale Air Quality (CMAQ) model.
18 A monthly emission inventory of six metals - Fe, Al, V, Ni, Zn, and Cu - from land anthropogenic, ship, and dust sources in
19 East Asia (0-55°N, 85-150°E) in 2017 was developed. Most metals came mainly from land-based sources, contributing over
20 80%. The annual marine atmospheric deposition fluxes of Fe, Al, V, Ni, Zn, and Cu were 9614, 15000, 102, 84, 171, 88 $\mu\text{g}\cdot\text{m}^{-2}$
21 ², and soluble deposition fluxes were 646.8, 1799.6, 43.3, 36.3, 118.4, 42.9 $\mu\text{g}\cdot\text{m}^{-2}$, respectively. Contributions of each source
22 for trace metals varied in emissions, atmospheric concentrations, and depositions. Dust source, as a main contributor of Fe and
23 Al, accounted for a higher proportion of emissions (~90%) than marine deposition fluxes (~20%). However, anthropogenic
24 sources have larger shares of marine deposition flux compared with emissions. The deposition of Zn, Cu, and soluble Fe in
25 East Asian seas was dominated by land anthropogenic sources, while V and Ni were dominated by shipping. The seasonal
26 gridded data and the identification of the dominant source of metal deposition offer a foundation for dynamic assessments of
27 the marine ecological effects of atmospheric trace metals. This study also implies the importance of potential co-synthesis and
28 complementation effects of multiple trace elements deposited into marine ecosystems.

29 1 Introduction

30 Trace metals have been the focus of marine biogeochemical studies for half a century. Trace metals (iron, cobalt, nickel,
31 copper, zinc, manganese, cadmium, lead, and rare earth elements, among others) are present in seawater at very low
32 concentrations, typically in the $\text{pmol}\cdot\text{L}^{-1}$ to $\text{nmol}\cdot\text{L}^{-1}$ range (Morel and Price, 2003). During the evolution of life, transition



33 metals play a crucial role in many biochemical functions. It is widely documented that transition trace metals are essential
34 nutrients for marine biota, such as Fe, Zn, Cu, and Ni (Butler, 1998; De Baar et al., 2018; Whitfield, 2001). Trace metals are
35 involved in nitrogen and carbon fixation by marine phytoplankton and their mechanism of action is to regulate the expression
36 of biological enzymes (Bonnet et al., 2008; Browning et al., 2017; Mackey et al., 2015; Morel et al., 1994; Nuester et al., 2012;
37 Rodriguez and Ho, 2014; Schmidt et al., 2016; Shaked et al., 2006; Sunda, 2012; Tortell et al., 2000; Wuttig et al., 2013a;
38 Wuttig et al., 2013b). Atmospheric deposition, seafloor hydrothermal upwelling, land-based sediment and riverine inputs, and
39 remineralization of the oceanic substrate are important sources of marine metals (Longhini et al., 2019; Yang et al., 2019). It
40 has been shown that the source of atmospheric deposition is important for some elements in seawater, e.g., global atmospheric
41 deposition of copper is comparable to or even higher than riverine inputs (Little et al., 2014; Takano et al., 2014) and that
42 atmospheric deposition can carry elements to more remote seas compared to riverine inputs (Yamamoto et al., 2022).

43 Atmospheric aerosols originate from both natural and anthropogenic sources. Aerosols originating from natural sources
44 (e.g., dust storms, volcanic eruptions, wildfires) differ significantly in their fluxes, composition, and properties from those
45 produced by human activities (e.g., industrial emissions, transportation, mining, agriculture) (Baker and Jickells, 2017; Barkley
46 et al., 2019; Hamilton et al., 2022; Ito et al., 2021; Shi et al., 2023; Zhang et al., 2022). Aerosols from natural sources have
47 high deposition fluxes and broad deposition ranges, especially for Al and Fe, but generally have low solubility (Baker et al.,
48 2020; Mahowald et al., 2005; Shi et al., 2015). By contrast, aerosols emitted from anthropogenic sources are characterized by
49 high temperatures and small particle sizes (Bowie et al., 2009; Chen et al., 2012; Li et al., 2017; Oakes et al., 2012), and
50 contains more soluble metallic elements (Yamamoto et al., 2022; Zhang et al., 2024). To accurately assess the biogeochemical
51 impact of the atmospheric input, atmospheric particulate species should be determined for the bioavailable soluble fraction
52 rather than only for the total concentrations or depositions (Birmili et al., 2006; Hsu et al., 2010). Therefore, emissions of
53 anthropogenic sources, although not as high as those from natural sources, are still of great concern. Anthropogenic sources
54 can be subdivided into land-based sources and shipping sources. Emissions of ships can be transported to remote sea areas
55 where land-based aerosols rarely reach. With the development of a booming shipping industry, their contribution to metal
56 deposition should not be ignored, particularly for V and Ni, which are considered the most abundant trace metals in heavy ship
57 fuel oils (HFO) (Celo et al., 2015; Corbin et al., 2018).

58 The spatial distribution of metal emissions from ship and anthropogenic sources, contrasts with that of dust (Mahowald et
59 al., 2018). Matsui et al. suggested that anthropogenic iron may dominate the total deposition flux of soluble iron and its
60 variability in the Anthropocene, especially over southern oceans (mid-latitudes and high-latitudes), where the ocean
61 biogeochemistry is likely to be iron limited (Matsui et al., 2018). When we focus on specific ocean areas, such as iron limited
62 ocean, and possibly other metals in the future, it is important to have a clear understanding of the dominant sources in the
63 ocean.

64 Current studies on metal emission inventories mainly focused on land-based emission sources (Bai et al., 2021; Tian et al.,
65 2015; Wang et al., 2016). The inventories including high-resolution ship sources only covered a limited number of metals such
66 as V and Ni (Zhai et al., 2023; Zhao et al., 2021a), yet the contribution of shipping to other metals should also be considered.



67 Previous studies about the concentration and deposition flux of metals were done by site observations and source
68 apportionment by statistical methodologies (Fu et al., 2023; Okubo et al., 2013; Pan and Wang, 2015; Pan et al., 2021; Tao et
69 al., 2016; Tao et al., 2017; Wei et al., 2014; Zhang et al., 2024). Due to limitations in the location of the observation sites,
70 these studies were unable to provide data over a wide area of the ocean and there was uncertainty in confirming the source
71 based on statistical methods. Current model-based simulations of gridded concentrations, deposition fluxes, and distinguishing
72 between sources were mainly focused on Fe (Matsui et al., 2018; Yamamoto et al., 2022). The broader regional scale study by
73 air quality model was few maybe due to the shortage of emission inventories of trace elements. The emission inventories,
74 including metals with marine ecological effects and metals representative of dust and ship sources, need to be developed.
75 Additionally, the atmospheric transport processes of these metals and their deposition fluxes to the ocean remain to be studied.

76 In this study, we established an emission inventory of six metal elements (Fe, Al, V, Ni, Zn, Cu) from three major emission
77 sources, namely, land anthropogenic, ship and dust sources, in the East Asian region (0-55°N, 85-150°E) in 2017. The aerosol
78 module in the Community Multiscale Air Quality (CMAQ) model was modified to simulate the concentration, dry and wet
79 deposition fluxes of the metallic elements, and calculated the soluble metal deposition fluxes. In addition, we quantified the
80 contribution of each source to the emissions and concentrations of metal elements in East Asia and analyzed the sources of
81 deposited metals in different sea areas.

82 **2 Materials and Methods**

83 **2.1 Description of the Modelling System**

84 The CMAQ is a widely used air quality model that encompasses a wide range of complex atmospheric physicochemical
85 processes. This study modeled metal concentrations and dry and wet deposition fluxes using the CMAQ version 5.4. The
86 multi-pollutant code in the aerosol module and the in-line dust emission module of CMAQ v5.4 were modified to add metallic
87 elements as modeling variables. In the revised version of the CMAQ model, it was assumed that these 6 metallic elements
88 were considered as inert chemical constituents in aerosols, which can participate in atmospheric physical processes such as
89 diffusion, advection, and deposition, but do not participate in any atmospheric chemical reactions. Specific modifications are
90 described in the Supporting Information (Text S1).

91 The CMAQ model configuration utilized AERO7 for the aerosol module (Xu et al., 2018) and CB6r5 for the gas-phase
92 mechanism (Amedro et al., 2020), including detailed halogen chemical components (Sarwar et al., 2019) and DMS (Lana et
93 al., 2011; Zhao et al., 2021b). Initial and boundary conditions for the simulation domain were established based on seasonal
94 average hemispheric CMAQ output from the CMAS data repository (Us, 2019). Meteorological fields were generated using
95 the Weather Research and Forecasting (WRF) model version 4.1.1, with initial and boundary conditions sourced from the 6-
96 hour temporal resolution National Centers for Environmental Prediction (NCEP) Final Operational Global Analysis dataset.
97 The physics schemes are listed in the Supporting Information (Text S2).



98 In this study, three scenarios were carried out to investigate the whole process from emission to atmospheric concentration
99 to deposition in the sea and the effects of different emission sources on atmospheric concentration and deposition fluxes of
100 metals. One scenario included three emission sources: land anthropogenic, ship and dust sources. Another scenario included
101 only land anthropogenic and dust sources. The other scenario included only land anthropogenic and ship sources. The
102 contributions of ship and dust sources to metal concentrations and deposition fluxes were extracted based on the zero-out
103 method, i.e., two runs with and without ship or dust emissions. And the impact of land anthropogenic sources was further
104 calculated. Each simulation was conducted for the month of January, April, July, and October of 2017 with a 5-day spin-up
105 period, representing winter, spring, summer, and autumn, respectively. The simulation domain covers East Asia and most of
106 the East Asian Seas, as shown in Fig. S1, discretized with a horizontal grid resolution of 36 km and 27 vertical layers between
107 the surface and 100 hPa, and the surface layer thickness was ~40 m.

108 2.2 Methodology of Metal Emission Inventory

109 In this study, metal emission sources were categorized into land anthropogenic, ship, and dust sources. The general
110 methodology for calculating land anthropogenic emissions of metals was to multiply each source of PM emissions by the
111 fraction of the metal content in PM. Each source category of PM emissions was provided by the Emissions Database for Global
112 Atmospheric Research (EDGAR) emission inventories (Crippa et al., 2020) (global, $0.1 \times 0.1^\circ$ resolution), and corresponding
113 source-specific speciation profiles were created based on the SPECIATE v5.1 database (Bray et al., 2019; Simon et al., 2010)
114 The same approach was used in previous metal emission inventories (Gargava et al., 2014; Kajino et al., 2020; Reff et al.,
115 2009; Xuan, 2005; Ying et al., 2018).

116 Ship sources metal emission inventory was established by a bottom-up approach based on the automatic identification
117 database (AIS) of ships (Yuan et al., 2023; Zhao et al., 2020). Parameters such as power-based emission factors (in $\text{g}\cdot\text{kWh}^{-1}$)
118 are listed in the Supporting Information (Table S1 and S2) and the low load adjustment multipliers can be found in the previous
119 studies (Chen et al., 2017; Fan et al., 2016). More information on the emission inventories can be found in the Supporting
120 Information (Text S3).

121 Dust emissions of trace metals were generated from in-line modules during the CMAQ run. We modified the in-line
122 windblown dust module to incorporate metal species, facilitating its concurrent operation with the MODIS land cover data.
123 For the dust speciation factor, we adjusted the fine and coarse mode mass fractions of metal species based on a comprehensive
124 literature review. The detailed findings of the literature review, along with the ultimately modified values, are presented in
125 Table S3.

126 2.3 Calculation of soluble metal deposition fluxes

127 In this study, the soluble fraction of the metal deposition flux was roughly calculated by multiplying the deposition flux
128 obtained from the CMAQ simulation by the solubility of the metal, which has also been used in previous study (Liu et al.,
129 2022; Zhang et al., 2024). The solubility of metals is closely related to the source (Chester et al., 1993). Kurisu et al. analyzed



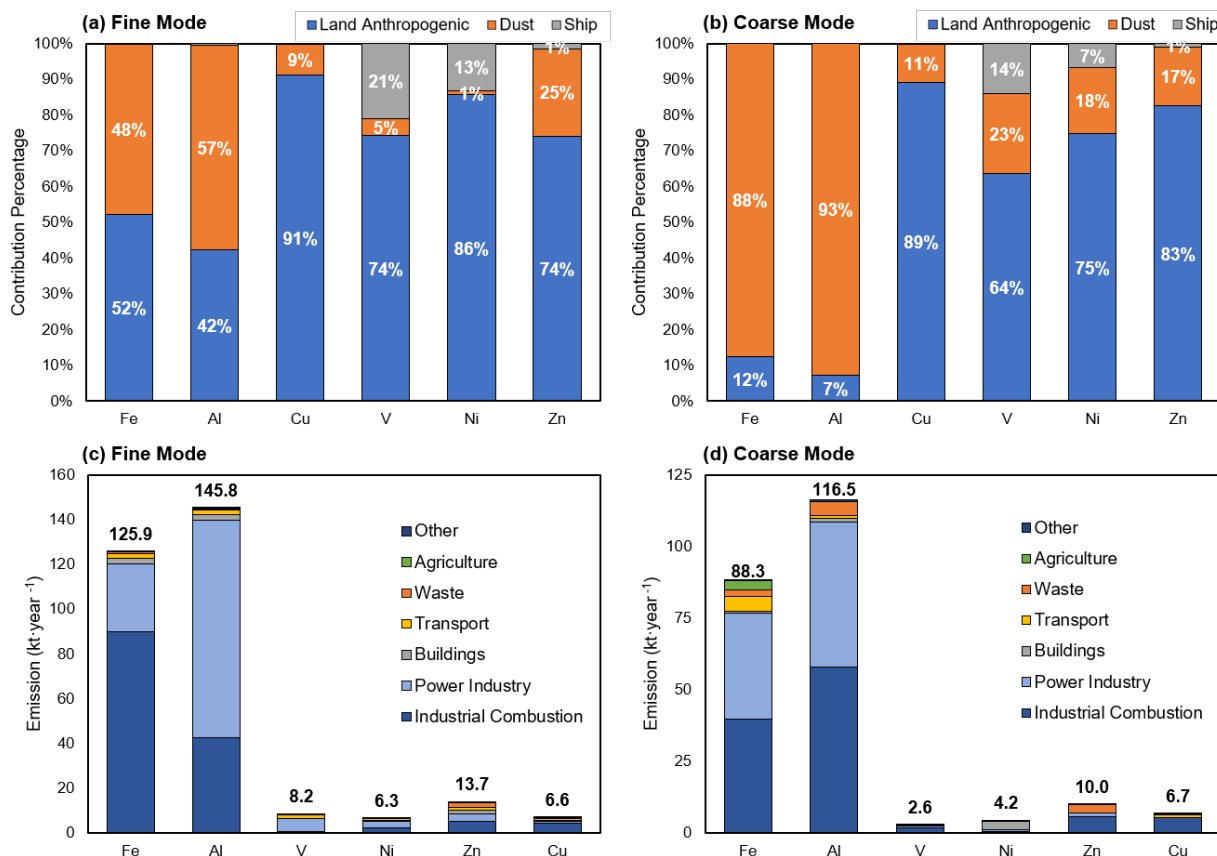
130 both dust and anthropogenic iron concentrations in total and soluble iron samples using a stable iron isotope source
131 apportionment method and showed that the dust iron solubility in the northwestern Pacific Ocean ranged from 0.9 ~ 1.3%
132 (dust-contributed soluble Fe divided by dust-contributed total Fe) and 11% for anthropogenic Fe solubility (anthropogenic-
133 contributed soluble Fe divided by anthropogenic-contributed total Fe) (Kurusu et al., 2021). However, a large number of
134 observations reported samples with iron solubility in the marine atmosphere exceeding 10% (Gao et al., 2013; Shi et al., 2013;
135 Sholkovitz et al., 2012), which illustrates the fact that a rough classification of sources into dust and anthropogenic sources is
136 not sufficiently plausible and that sources of emissions of highly soluble metals such as shipping, for example, need to be
137 considered as well (Ito, 2015). This study distinguished the contribution of different sources to the deposition flux of metals,
138 providing the possibilities for considering the distinct solubilities of metals from various sources. Given that current studies
139 primarily focused on Fe, obtaining solubility data for other metals from different sources proved challenging. The solubility
140 adopted in this study is shown in Table S4, which differentiated between fine and coarse modes and three emission sources
141 for Fe, and only two modes for the other metals.

142 **3 Results and Discussion**

143 **3.1 Emission Inventory**

144 **3.1.1 Contributions of Various Sectors**

145 This study assessed the relative contribution of the three sources to metal emissions and then further specified emissions
146 from land anthropogenic sources. As shown in Fig.1, for the fine mode of six metals, emissions originating from land
147 anthropogenic sources were much more significant than those from ship or dust sources, with relative contributions largely
148 exceeding 50% and peaking at 91.2%. The emissions from ship sources was not large overall, but the relative contribution to
149 fine mode V and Ni could reach 20.9% and 13.3%, which is similar to the results of previous studies on ship emissions (Yuan
150 et al., 2023; Zhao et al., 2021a). Dust substantially released Fe and Al in coarse mode (accounting for 88% and 93% of the
151 coarse mode emissions, respectively), while showing rather low contribution to other metals, which was related to the content
152 of metallic elements in soil minerals. Monthly emission statistics for both land anthropogenic and ship sources are detailed in
153 Table S5-S7. Land anthropogenic sources showed higher emissions of Fe and Al elements, amounting to 208.1 and 242.2
154 kt·year⁻¹ respectively. In contrast, V and Ni showed a lesser degree of impact from land anthropogenic activities, with values
155 of 8.2 and 9.4 kt·year⁻¹. V showed the highest fine and coarse mode ratio of 4.6, while Cu showed a ratio of 1.1. According to
156 Table S5-S7, the overall quantity of metals emitted by ships was predominantly higher in summertime (July and August) and
157 wintertime (November and December), while it was relatively lower in September. In terms of land anthropogenic sources,
158 there were no significant monthly variation.



159

160 **Figure 1: Relative contributions of land anthropogenic, ship, and dust sources to fine mode (a), coarse mode (b) emissions of the six**
 161 **metals (Fe, Al, V, Ni, Zn, Cu); stacked histograms of the absolute contributions of the seven emission sectors of land anthropogenic**
 162 **sources to fine mode (c), coarse mode (d), with the numbers representing the total emissions from all anthropogenic emission sectors.**

163 The predominant sources of emissions, specifically land anthropogenic sources, were further classified into seven categories
 164 according to EDGAR, namely Industrial Combustion, Power Industry, Buildings, Transport, Waste, Agriculture and Other
 165 (Figs.1c and 1d). For all six metals, both the Power industry and Industrial Combustion sources emerged as the prominent
 166 contributors, collectively accounting for more than 50% of the total land anthropogenic emissions. The emissions of Fe
 167 originating from industrial combustion were the largest, amounting to 129.5 kt·year⁻¹, with the fine mode accounted for 69.4%.
 168 The emissions of Al from the power industry were significant, amounting to 148.0 kt·year⁻¹, with the fine mode accounted for
 169 65.7%. In addition, the waste sector made a substantial contribution to Zn with 5.0 kt·year⁻¹, which was comparable to the 4.6
 170 kt·year⁻¹ contributed by the power industry. And the metals emitted from the waste sector were mainly in coarse mode, the
 171 proportion of coarse mode was more than 80%, except for Cu (24.8%) and Zn (55.9%).

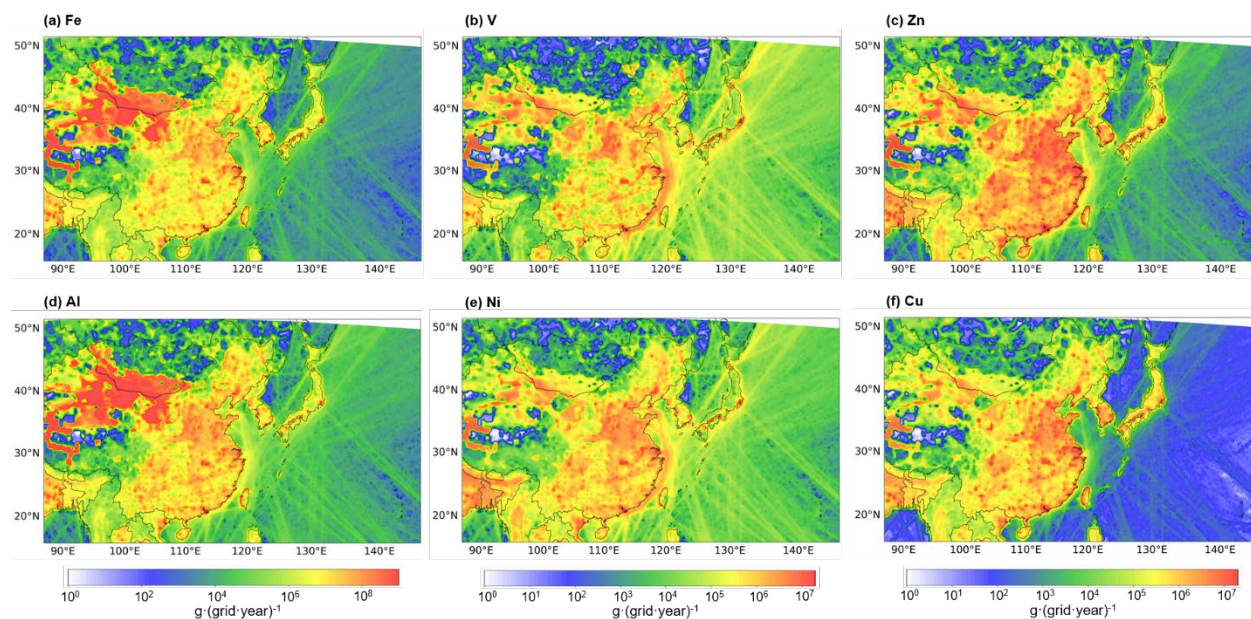
172 Several studies on metal emission inventories (refer to Table S8) are accessible for conducting comparative analyses. In the
 173 context of land anthropogenic sources, the emissions of Ni were reported as 3,395.5 tons, Zn as 22,319.6 tons, and Cu as
 174 9,547.6 tons in China in 2012 (Tian et al., 2015). Additionally, V emissions, inclusive of land anthropogenic and dust emissions,



175 were documented as 11,505.04 tons in China in 2017 (Bai et al., 2021). In this study, the corresponding values (ensuring
176 consistency of emission sources and areas) were 5,494.5 tons for Ni, 13,407.2 tons for Zn, 6,578.9 tons for Cu, and 11,093.7
177 tons for V in 2017. In terms of subdivided emission sectors, solid waste contributions were 0.3, 43.5, 1790.7, and 382.4
178 tons·year⁻¹ for V, Ni, Zn, and Cu, respectively (Bai et al., 2021; Wang et al., 2017b), and 0.6, 27.9, 2194.0, and 185.6 tons·year⁻¹
179 ¹ in this study. The Iron and Steel sector emitted 79.6 and 105.0 tons·year⁻¹ of V and Ni (Bai et al., 2021; Wang et al., 2016),
180 compared to 109.2 and 196.0 tons·year⁻¹ in this study. The ship emissions of V and Ni in East Asia in 2015 reported by Zhao
181 et al. were 1329.8 and 580.4 tons/year (Zhao et al., 2021a), while in this study, they were 1,802.6 and 854.8 tons·year⁻¹, with
182 an acceptable range of differences. Considering the different base years of the inventories and the different types of
183 anthropogenic sources covered, results of this study were consistent with previous studies overall.

184 3.1.2 Spatial distribution of metal emissions

185 For the entire simulation area, the emissions of the Fe, Al, V, Ni, Zn, and Cu from all sources were 1677.6, 3354.3, 12.9,
186 12.6, 27.1, 14.4 kt in 2017, respectively. In the context of the modeled land area, China was found to release substantial
187 amounts of Fe, Al, V, Ni, Zn, and Cu, totaling 141,919.9, 154,642.0, 6,673.5, 6,586.8, 16,794.1, and 9,523.7 tons·year⁻¹,
188 respectively. Beyond China, significant emissions were found in the coastal cities of Japan and South Korea, as well as in
189 Southeast Asian regions. Specifically, Japan and South Korea contributed 6,239.5, 4,545.2, 190.7, 197.3, 538.8, and 424.6
190 tons·year⁻¹ to the six metals, respectively. The emissions from India were 37,717.7, 54,039.0, 1,059.0, 2,030.0, 3,055.2, and
191 1,756.7 tons·year⁻¹, respectively. Meanwhile, the emission from Southeast Asia were 6,655.3, 10,632.1, 268.8, 752.9, 812.8,
192 and 445.8 tons·year⁻¹. Significantly emissions in the North China Plain, the Yangtze River Delta, the Pearl River Delta, and
193 Central China can be attributed to dense human activity levels in these regions, as reported by previous study (Bai et al., 2021).
194 Notably, the dust source regions of East Asia, namely the Taklamakan Desert and the Mongolian Plateau, showed remarkable
195 emissions of Fe and Al, surpassing those of densely populated and economically developed regions by an order of magnitude
196 or more.



197

198 **Figure 2: Girded metal emissions from all sources for the year 2017 (36 km ×36 km resolution; units, grams per year per grid cell,**
199 **including land anthropogenic, ship, and dust sources). Fe (a), V (b), Zn (c), Al (d), Ni (e), Cu (f). See Table S5-7 for detailed emission**
200 **data information.**

201 Within the marine domain, the emission trajectories of V and Ni were more substantial than the rest of the metals, as Fig.2
202 illustrated. In the coastal waters of eastern China, ship activities are dynamic, creating a linear high-emission zone in areas
203 with dense shipping routes, and the emissions of V and Ni brought by ships were comparable to the contribution of land
204 anthropogenic sources. By contrast, the emissions of the remaining four metals in the marine area were notably lower than
205 those in the land area. Furthermore, ships represent in-site sources of marine pollution, their emission footprint covers the vast
206 expanse of the Pacific Ocean, highlighting the importance of considering ship sources in emission inventories.

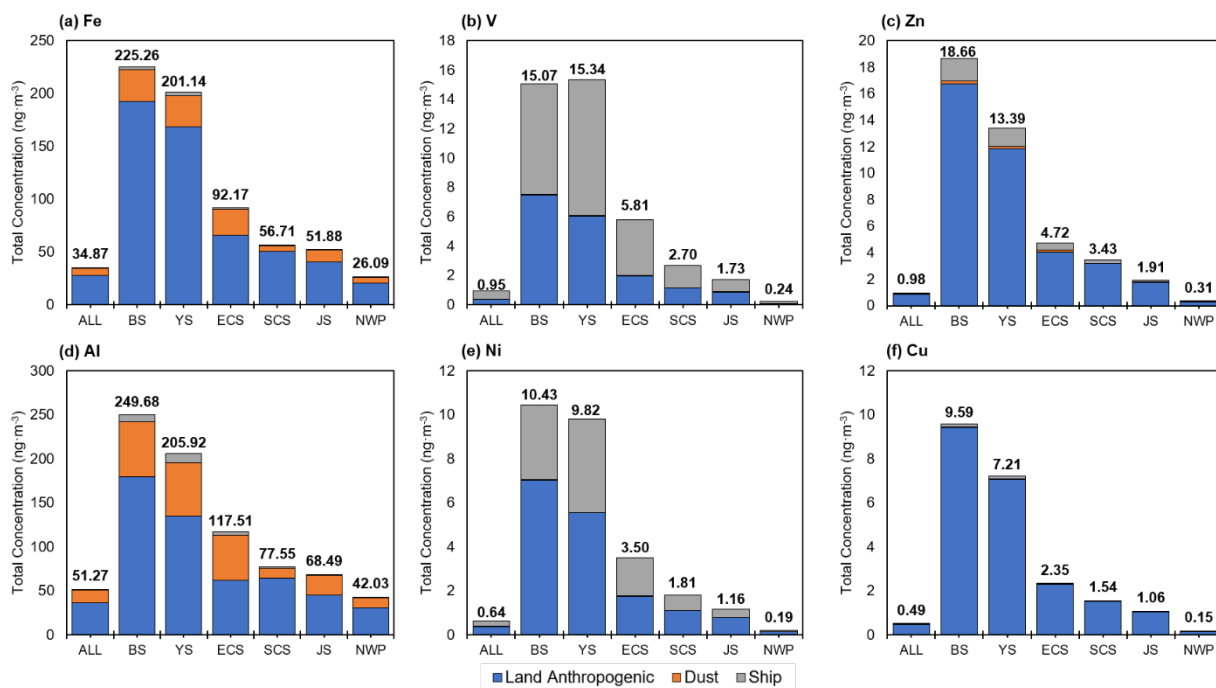
207 3.2 Contributions of different sources to marine atmospheric metal concentrations and deposition fluxes

208 3.2.1 Contributions of different sources to marine atmospheric metal concentrations

209 Based on the emission inventory of metallic elements established in Sect.3.1, the concentrations of metals in the sea areas
210 and the contributions of different sources were simulated by CMAQ model. Overall, the metallic concentrations in sea areas
211 were 34.9, 51.3, 1.0, 0.6, 1.0, and 0.5 ng·m⁻³ for Fe, Al, V, Ni, Zn, and Cu, respectively. Concentrations in the Bohai Sea (BS)
212 and the Yellow Sea (YS) were significantly higher than those in the other seas, about 5-20 times higher than the sea-wide
213 average (Fig.3). The BS demonstrated the highest concentrations of five metallic elements, Fe, Al, Ni, Zn, and Cu, at 225.3,
214 249.7, 10.4, 18.7, and 9.6 ng·m⁻³, respectively. The YS showed a notably higher concentration of V (15.34 ng·m⁻³), which was
215 attributed to dense ship activities in the marginal sea of China. Dust sources predominantly influenced the concentrations of
216 Fe and Al, accounting for 17.9% and 28.5%, on the sea-wide average, and their contributions to the remaining four elements



217 were far less than those from land anthropogenic or ship sources. Particularly within the East China Sea (ECS), dust sources
 218 played a more significant role, contributing 26.9% and 44.0% to Fe and Al concentrations, respectively. Ship sources mainly
 219 contributed to the concentrations of V and Ni in the sea area, with average contribution shares of 56.4% and 37.8%, and can
 220 reach 65.7% and 49.3% in the ECS, respectively. Land anthropogenic sources were the most important contributors to the sea
 221 level concentrations of most of the metal elements, excluding V, with an average contribution of 42.7%. Notably, for Cu,
 222 which is not a major metal element emitted from ships and whose content in dust particles is relatively small, the contribution
 223 from anthropogenic sources was as high as 97.6%. The concentration of Fe was 201.1 $\text{ng}\cdot\text{m}^{-3}$ in the YS and 92.17 $\text{ng}\cdot\text{m}^{-3}$
 224 in the ECS, and the contribution of land anthropogenic sources to the Fe concentration was 71.6% in the ECS, similar with the
 225 values reported by previous study (Zhang et al., 2024). Additionally, Table S9 presents a comparison between the metallic
 226 element concentrations in the East Asian land region and the simulation results derived from this study.



227

228 **Figure 3: Contributions of annual mean concentrations of metallic elements in different sea areas from land anthropogenic, ship,**
 229 **and dust sources, Fe (a), V (b), Zn (c), Al (d), Ni (e), Cu (f) (units: $\text{ng}\cdot\text{m}^{-3}$), with the numbers at the top of the stacked bar charts**
 230 **representing the total annual mean concentrations from the three major sources.**

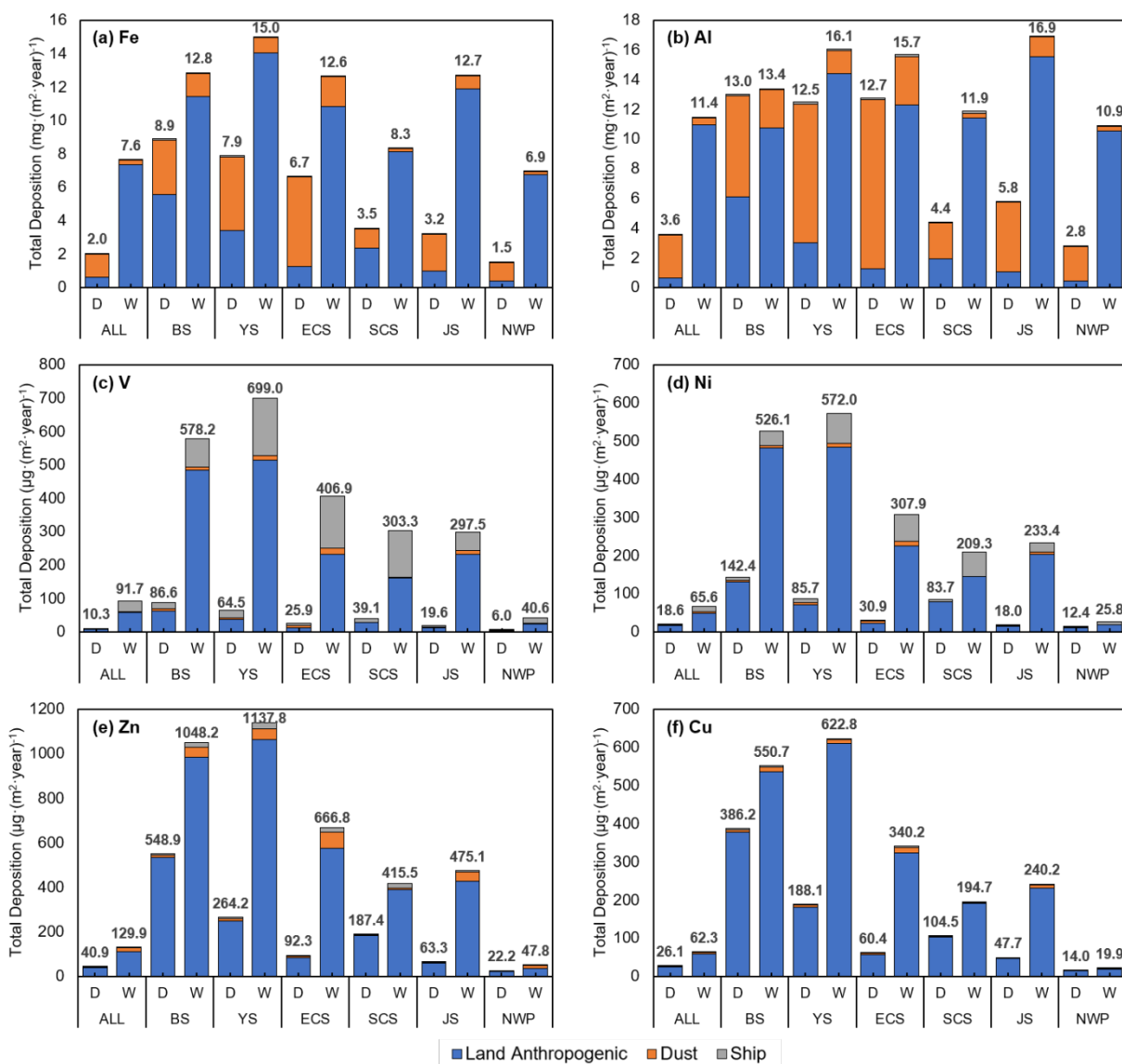
231 Land anthropogenic, ship, and dust sources presented discernible differences in both absolute and relative contributions of
 232 metal elements across diverse sea areas. Moreover, metallic element concentrations originating from these three sources
 233 showed distinct spatial distributions. As illustrated in Fig.S2, all the six metal concentrations attributed to land anthropogenic
 234 sources were notably higher in coastal areas, particularly in the proximity of China and Korea. Because land anthropogenic
 235 metals are mainly transported by diffusion and advection rather than strong weather processes, which is different from dust
 236 sources. Asian dust storms occur annually in late winter and spring in the main dust regions of the Gobi Desert, Taklamakan



237 Desert, and Loess Plateau (Hsu et al., 2010), and studies have shown that the outbreak of Asian dust storms is often associated
238 with the Mongolian cyclones during spring (Gui et al., 2022). This atmospheric phenomenon results in the transport of metal
239 particles from natural dust sources to more open sea areas, rather than being confined to coastal areas, and these metal particles
240 show a spatial distribution pattern following the trailing flow of the cyclone. Due to the higher contents of Fe and Al elements
241 in soil, concentrations of Fe and Al resulting from dust were 2-3 orders of magnitude higher than those of the other four metals.
242 Metal concentrations from ship sources were predominantly distributed around busy shipping routes, with higher
243 concentrations within the 200 nautical miles (nm) range of East Asian countries. However, high concentration values were
244 noted at a certain distance from the coastline, distinct from the concentration distribution of land anthropogenic sources.

245 **3.2.2 Contributions of different sources to marine atmospheric metal deposition fluxes**

246 The influence of the three emission sources on metal deposition fluxes and concentrations across the sea areas displayed
247 distinctive characteristics. As depicted in Fig.3, the concentrations of six metal elements over the BS and the YS markedly
248 surpassed those recorded in other seas, and were even 6-60 times higher than the concentrations over the open Northwest
249 Pacific Ocean (NWP). However, the deposition fluxes of metal elements over proximate coastal areas, including the BS, the
250 YS, the ECS, the South China Sea (SCS), and the Sea of Japan (JS), showed relatively insignificant differences, although the
251 BS and the YS still displayed the highest fluxes (Fig.4). It can be seen that the spatial distribution of metal deposition in the
252 seas was broader than that of metal concentrations. Table S10 presents the comparison of the stimulated deposition fluxes of
253 the metals in this study with existing observation-based studies on metal deposition fluxes. Given that the existing studies
254 focused more on the land area, this study employed land deposition flux data for comparison. The deposition fluxes of the six
255 metals were within the range of the existing studies, validating our results.



256

257 **Figure 4: Contributions of land anthropogenic, ship and dust sources to annual dry and wet deposition fluxes of metallic elements**
 258 **(represented by D and W, respectively, in the figures) in different marine areas, Fe (a), Al (b), V (c), Ni (d), Zn (e), Cu (f) (units:**
 259 **mg·m⁻²·year⁻¹ for Fe and Al, µg·m⁻²·year⁻¹ for V, Ni, Zn, Cu), and the numbers above the stacked bars represent the total annual**
 260 **dry or wet deposition fluxes from the three major sources.**

261 Particulate elements are removed from the atmosphere through dry and wet deposition processes, and wet deposition is
 262 generally more important than dry deposition in marine areas (Mahowald et al., 2005). At the marine scale, wet deposition
 263 fluxes were greater than dry deposition for all six metal elements, which is in line with previous findings (Connan et al., 2013;
 264 Gao et al., 2013; Zhang et al., 2024). The dry and wet deposition ratios (i.e., dry deposition flux/wet deposition flux) of Fe, Al,
 265 V, Ni, Zn, and Cu were 0.26, 0.31, 0.11, 0.28, 0.32, and 0.42 across the entire study sea area, respectively. Dry deposition flux



266 is a function of atmospheric concentration and particle dry deposition velocity. Wet deposition removes airborne particulate
267 elements via precipitation scavenging, which includes in-cloud and below-cloud scavenging (Cheng et al., 2021). The size
268 distribution of metals in atmospheric aerosols is a key factor influencing the differences between wet and dry deposition flux.
269 Sakata and Asakura indicated that metals associated with coarse particles ($> 2.5 \mu\text{m}$ in diameter) have shorter atmospheric
270 lifetimes due to gravitational settling and inertial deposition, which easily govern dry deposition (Sakata and Asakura, 2011).
271 Fine particulate matter, on the other hand, is more likely to serve as condensation nuclei for wet deposition. Dust sources,
272 typically characterized by large particle sizes, are consequently more readily removed from the atmosphere through dry
273 deposition during atmospheric transport. The fine mode proportion of the six metals from both land anthropogenic and ship
274 sources were, in descending order, V (82%), Ni (62%), Fe (60%), Zn (60%), Al (59%), and Cu (51%), and anthropogenic
275 sources contributed more than dust sources. As a result, these sources contributed predominantly to metal deposition in the sea
276 through wet deposition processes. The difference in particle size and behavior highlights the complex interplay between
277 source-specific attributes and deposition mechanisms, influencing the fate of metals in the atmosphere and their subsequent
278 deposition in the ocean.

279 The spatial distribution of annual deposition fluxes of six metals in the sea were illustrated in Fig.S3. Over the whole sea
280 area, the annual deposition fluxes of Fe, Al, V, Ni, Zn, and Cu were 9,613.8, 15,000.0, 101.9 84.2, 107.8, and 88.3 $\mu\text{g}\cdot\text{m}^{-2}\cdot\text{year}^{-1}$
281 ¹, respectively, in which the highest values of deposition fluxes reached 260.0, 246.8, 2.7, 3.0, 16.9, 11.0 $\text{mg}\cdot\text{m}^{-2}\cdot\text{year}^{-1}$. The
282 deposition of Fe and Al in the sea showed a wider spatial extent compared to other four metals, particularly in the NWP.
283 Combined with Fig.S2, it can be hypothesized that this phenomenon was caused by dust sources, as metallic particulate matter
284 was transported and deposited into the more open ocean along with intense weather processes like cyclone and cold front (Li
285 and Chen, 2023). The deposition of V, Ni, Zn, and Cu, was primarily distributed in offshore waters, such as the BS, the YS,
286 and the JS, as well as within the 100 nm range in eastern China. The deposition fluxes of V were high in the 200 nm range in
287 eastern China, which is related to the ship activities, as reported by previous study (Zhao et al., 2021a).

288 3.2.3 Estimation of Deposition Flux of Soluble Metals in Maritime Areas

289 Utilizing the calculation methods in Sect.2.3, the detailed outcomes of these calculations were provided in Table 1. In this
290 context, the soluble iron deposition flux was calculated separately for each of the three sources and then summed to obtain the
291 total soluble deposition flux. Land anthropogenic, ship, and dust sources contributed 600.0, 10.6, and 2.9 $\mu\text{g}\cdot\text{m}^{-2}\cdot\text{year}^{-1}$ of
292 soluble iron in the fine mode and 10.9, 0, and 23.3 $\mu\text{g}\cdot\text{m}^{-2}\cdot\text{year}^{-1}$ of soluble iron in the coarse mode, respectively. Based on
293 this method, the final solubility of iron obtained in this study ranged from 2% to 22%, which is comparable to the results of
294 previous studies (Alexander et al., 2009; Kurisu et al., 2021; Shao et al., 2019).

295 **Table 1: Marine deposition fluxes of soluble metals in fine and coarse particulate forms (Units: $\mu\text{g}\cdot\text{m}^{-2}\cdot\text{year}^{-1}$)**

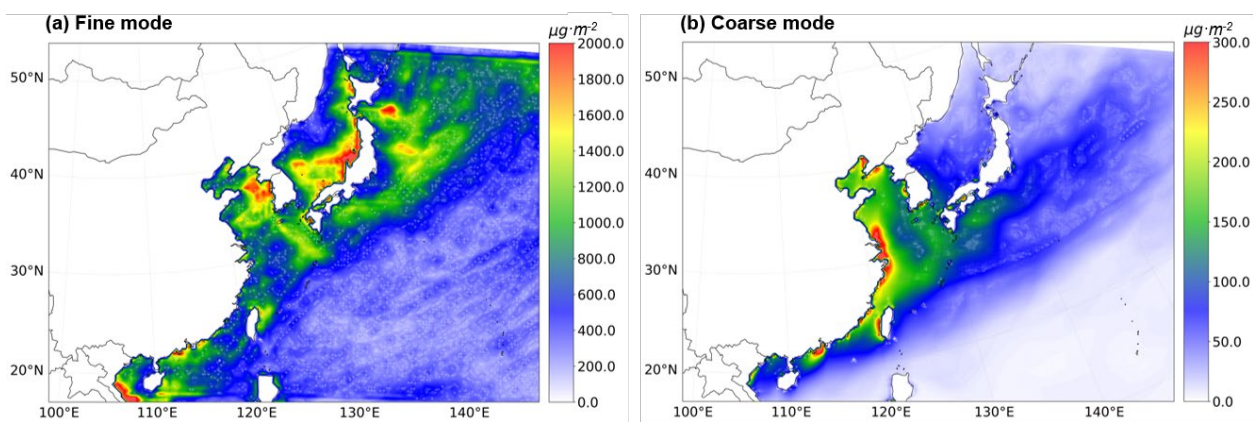
Cu	Fe*	Zn	V	Ni	Al
----	-----	----	---	----	----



Fine	26.5	612.6	83.6	39.6	30.3	1638.0
Coarse	16.4	34.2	34.8	3.7	6.0	161.6

296 *The soluble iron deposition flux was calculated separately for each of the three sources and then summed to obtain the total soluble
 297 deposition flux

298 Figure 5 illustrated the spatial distribution of fine and coarse mode soluble Fe deposition over different sea areas, and Fig.S4
 299 showed the absolute and relative contributions of the three sources to soluble Fe deposition over these areas. The spatial
 300 distribution displayed marked differences for different particle sizes. The deposition fluxes of fine-mode soluble iron were
 301 large throughout the ocean and varied less between seas. The highest deposition flux occurred in the YS (1114.6 $\mu\text{g}\cdot\text{m}^{-2}\cdot\text{year}^{-1}$)
 302 and the lowest occurred in the NWP (567.3 $\mu\text{g}\cdot\text{m}^{-2}\cdot\text{year}^{-1}$). Despite the relatively lower deposition flux in the NWP, it still
 303 exerted a noticeable impact on the NWP. In contrast, coarse-mode soluble iron was mainly distributed in marginal seas, and
 304 the depositional flux in the BS (220.3 $\mu\text{g}\cdot\text{m}^{-2}\cdot\text{year}^{-1}$) was ~ 9 times higher than that in the NWP (21.6 $\mu\text{g}\cdot\text{m}^{-2}\cdot\text{year}^{-1}$). Across
 305 the ocean, soluble iron deposition fluxes were greater in the fine-mode state than in the coarse-mode state, at 612.6 and 34.2
 306 $\mu\text{g}\cdot\text{m}^{-2}\cdot\text{year}^{-1}$, respectively. Fine-mode soluble iron was primarily contributed by land anthropogenic sources, with a relative
 307 contribution exceeding 94% across all marine regions. Its impact from dust was smaller than that from ship sources, and the
 308 contribution of ships to the Chinese Marginal Sea was in the range of 3-6%, which can reach 19.2% to the ECS during the
 309 summertime when ship activities are dynamic. Coarse-mode soluble iron was strongly influenced by dust, with its contributions
 310 reaching up to 85% in the NWP, as illustrated in Fig.S4.



311
 312 **Figure 5: Fine mode (a) and coarse mode (b) spatial distribution of soluble iron deposition fluxes throughout the year of 2017 (units:**
 313 **$\mu\text{g}\cdot\text{m}^{-2}\cdot\text{year}^{-1}$, including land anthropogenic, ship, and dust sources).**

314 On the one hand, aerosols emitted by anthropogenic sources are rich in acidic species such as NO_x and sulfur dioxide (SO_2),
 315 whereas aerosols of dust tend to contain a significant portion of carbonates (Böke et al., 1999), which are much less acidic
 316 than anthropogenically sourced aerosols (Ito et al., 2019). For trace metals, acidity affects solubility through insoluble minerals
 317 readily dissolving under acidic conditions relevant to atmospheric aerosol (Baker et al., 2021; Hamilton et al., 2023; Li et al.,



318 2017). On the other hand, smaller particles can undergo longer distance transport in the atmosphere. Along with particle aging,
319 metal morphology changes, and more metals dissolve. Besides, the emission of metals from anthropogenic sources was higher
320 in the fine mode than coarse mode. The above reasons collectively lead to a higher deposition flux of soluble iron in the fine
321 mode.

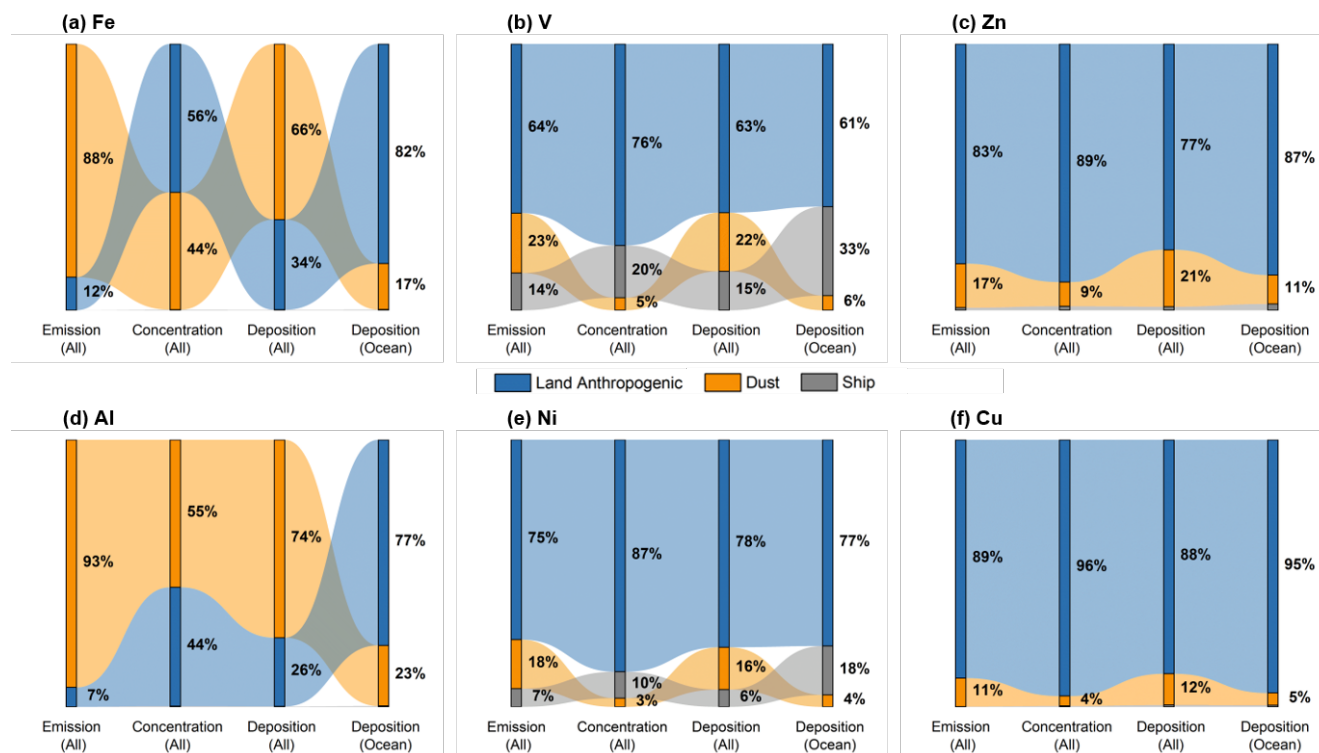
322 3.3 Sources and Sinks of Marine Metals

323 3.3.1 Emission-Concentration-Deposition

324 In Sect.3.1 and Sect.3.2, we discussed the contributions of the land anthropogenic, ship, and dust sources to the emissions,
325 atmospheric concentrations and deposition flux of six metal elements. This section focused on the source-sink patterns of metal
326 elements in maritime areas. Figure 6 illustrated the proportional contributions of the three major sources to the entire area (land
327 and ocean) emissions, concentrations, deposition, and maritime deposition of the six metals (percentages were calculated from
328 one specific source divided by total contribution of the three sources). It can be found that for the predominant emission metals
329 Fe and Al originating from dust sources, the contributions of dust sources to emissions far exceeded that of land anthropogenic
330 sources. However, as atmospheric transport processes occurred, the contribution of land anthropogenic sources became
331 significant and was comparable to the contribution of dust sources to atmospheric concentrations. In particular, the contribution
332 of land anthropogenic sources became dominant when focusing on marine deposition. For Fe, the contribution from land
333 anthropogenic sources was 12%, 56%, 34%, and 82% in the four stages from emissions to maritime deposition flux, similar
334 with results reported by previous study (Kajino et al., 2020). Similarly, for Al, the corresponding contributions were 7%, 44%,
335 26%, and 77%. The contributions from dust sources in maritime deposition flux (17% for Fe and 23% for Al) were lower than
336 those in emissions (88% for Fe and 93% for Al). Although dust particles typically have large particle size, making them more
337 likely to deposit during atmospheric transport, which explains why, for all metals, the contribution of dust sources in
338 concentrations was lower than that in emissions and in deposition fluxes over the entire modelled area. However, because the
339 dust source areas are mainly inland, such as Mongolia and northwestern China, the contribution of dust sources to metal
340 deposition in the sea was much less than that in the entire modelled area. Additionally, a portion of the dust particles were
341 transported to higher elevations or farther out to sea during strong weather events, beyond the modelled area of this study. This
342 could also lead to a lower contribution of dust sources to metal deposition in sea areas. It can be shown that dust sources were
343 not the most important contributors to metal deposition fluxes in the East Asian Seas. For metals such as V and Ni, the
344 contributions from ship sources in deposition flux (33% and 18% respectively) were larger than those in emissions (14% and
345 7% respectively) and in deposition over the entire modelled area (15% and 6%, respectively). This reaffirmed the importance
346 of ship sources when considering the metal deposition in the sea areas. Analyzing the contributions from the three sources
347 revealed that despite the presence of dust source areas and high dust emissions in East Asia, the impact of dust on marine
348 depositional fluxes was not as large as its impact on emissions. The contribution of land anthropogenic sources to maritime
349 deposition flux was generally higher than that to emissions, except for V, where ship sources had a greater impact on deposition



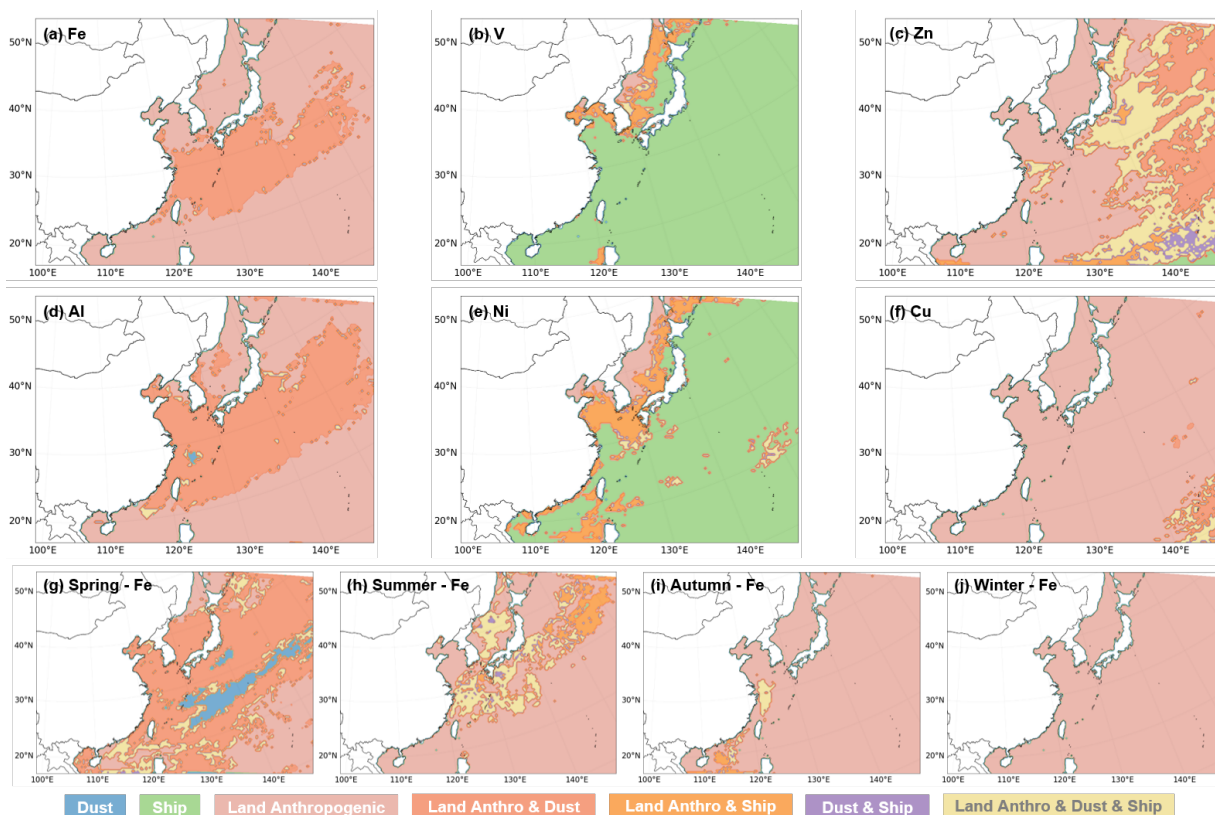
350 fluxes than on emissions. While it is true that dust sources contribute more metals, the impact of human activities on metal
 351 deposition is of greater concern when we focus on the East Asian seas.



352
 353 **Figure 6: Evolution of the relative contributions of the land anthropogenic, ship, and dust sources to emissions, annual mean**
 354 **concentrations, annual deposition fluxes, and annual oceanic deposition fluxes of metallic elements Fe (a), V (b), Zn (c), Al (d), Ni**
 355 **(e), Cu (f). (Emissions, annual mean concentrations, and annual deposition fluxes were for the entire modelled area, including land**
 356 **and sea, labelled "All" in the figure, and oceanic deposition fluxes for the ocean only, labelled "Ocean" in the figure).**

357 3.3.2 Dominant Maritime Regions for the Three Major Emission Sources

358 The identification of the dominant sea area for sources was established based on the contributions of the three major sources
 359 to the marine deposition flux of metals. For each ocean grid in this study, the contribution rate of a source was calculated by
 360 dividing the metal deposition flux attributed to that source by the total deposition flux of the metal, thereby obtaining the
 361 contribution rate for the specific grid. The criteria were employed as follows. If one source contributed more than 66.7%, it
 362 was considered to dominate the metal deposition flux of the grid. If both sources contributed more than 33.3%, with the
 363 remaining one contributing less than 33.3%, it was considered that the two sources jointly dominated the deposition flux of
 364 the grid. And in the absence of dominance by one or two sources, it was considered that the three major sources collectively
 365 influenced the metal deposition flux of the grid.



366

367 **Figure 7: The dominant source distributions of metal deposition fluxes in the ocean, Fe (a), V (b), Zn (c), Al (d), Ni (e), Cu (f); (g-j)**
368 **are the dominant source of the deposition fluxes of soluble Fe in spring, summer, autumn and winter seasons. (In this study, we**
369 **calculated the relative contributions of the metal sedimentation fluxes from the three major sources for each grid. A source was**
370 **considered to dominate metal deposition on the grid if its contribution was >67%, two sources were considered to jointly dominate**
371 **metal deposition on the grid if both sources contribute >33%, and three sources were considered to jointly dominate in the rest of**
372 **the cases).**

373 Based on the aforementioned calculation and criteria, the dominant sea areas for metal deposition fluxes from the three
374 major sources were depicted in Fig.7. For Fe, Al, Zn, and Cu, land anthropogenic sources dominated the deposition fluxes in
375 almost all offshore areas proximate to land. For V and Ni, a considerable range of metal deposition fluxes were dominated by
376 both land anthropogenic and ship sources in offshore areas near land, especially in the BS, the YS, and the JS. In the vast
377 majority of the open ocean area, the deposition of V and Ni was mainly dominated by ship sources. In contrast, for Fe and Al,
378 there were scarcely any regions where land anthropogenic and ship sources co-dominate, but in the ECS and the NWP, a large
379 range of metal deposition was co-dominated by both land anthropogenic and dust sources, similar with the previous result
380 (Matsui et al., 2018). For Cu and Zn, the area dominated by land anthropogenic sources was extensive, especially for Cu,
381 where land anthropogenic sources dominated the metal deposition fluxes in almost the entire ocean. Conversely, for Zn, areas
382 still existed where both dust and land anthropogenic sources dominate, alongside areas where the three major sources
383 collectively influenced the deposition fluxes in the western Pacific Ocean.



384 The main sources of six metallic elements were different, leading to the deposition of metallic elements in distinct oceanic
385 areas. Consequently, when assessing the ecological effects of a specific metal, it becomes particularly important to identify its
386 dominant emission sources. Mahowald et al. estimated that ocean primary productivity was enhanced by 6% due to the
387 doubling of desert dust which carried iron during the 20th century (Mahowald et al., 2010). When we combined this result on
388 dust sources along with our findings regarding the dominant source of soluble iron (see Figs.7g-7j) - the area of the East Asian
389 Seas dominated by anthropogenic sources of deposition was larger than that of dust sources - the resulting primary productivity
390 of the East Asian Seas may be more significant with the growing metal emissions from anthropogenic sources. Given that
391 different metal elements have distinct ecological effects in marine environments, it is crucial to consider their specific
392 implications. For example, the nutrient effect of Fe on marine primary productivity is a significant consideration (Bonnet et
393 al., 2008; Mackey et al., 2015; Mahowald et al., 2009; Schmidt et al., 2016; Yamamoto et al., 2022). For Cu, the focus may be
394 on its toxicity or synergistic effects with Fe on biophysiological processes (Guo et al., 2012; Wang et al., 2017a; Yang et al.,
395 2019; Zou et al., 2015). Zn, on the other hand, might be considered for its role in carbonic anhydrase and other biochemical
396 processes (Morel et al., 1994; Shaked et al., 2006; Tortell et al., 2000). Our identification of the main sources of metal
397 deposition in sea waters aids in investigating the potential ecological impacts.

398 **4 Conclusion**

399 Trace metals have a non-negligible impact on marine ecology, and their impact on marine productivity continues to be
400 explored. Due to the challenges of measuring atmospheric deposition fluxes in open seas, air quality models provide a solution
401 for this task. In this study, we established a monthly emission inventory covering six metal elements (Fe, Al, V, Ni, Zn, and
402 Cu) in the East Asian region (0-55°N, 85-150°E), incorporating land anthropogenic, ship, and dust sources. The CMAQ was
403 modified to assess the concentrations and deposition fluxes of metal species over the East Asian Seas and subsequently
404 estimated the soluble metal deposition fluxes, with a focus on the contributions of different sources across various sea regions.
405 We analyzed the evolutions in the relative contributions of the three sources to the six metals from source-emission, to sink-
406 deposition, and identified the dominant sources of deposition of the six metals in sea waters.

407 Throughout the year of 2017, emissions from all sources were 1677.6, 3354.3, 12.9, 12.6, 27.1, and 14.4 kt of Fe, Al, V, Ni,
408 Zn, and Cu, respectively. The contribution of land anthropogenic sources to metal emissions was significant, exceeding 60%
409 for most metals, except for Fe and Al in the coarse mode, where the contributions from dust sources (88% and 93%,
410 respectively) were larger. Ship sources contributed more to V and Ni than to the remaining metals, mainly in the fine mode.
411 China was an emission hotspot for metallic elements within the modelled land area, and regions with dynamic ship activity
412 were emission hotspots for metals in the modelled sea area. The annual concentrations of Fe, Al, V, Ni, Zn, and Cu in the sea
413 areas were 34.87, 51.27, 0.95, 0.64, 0.98, and 0.49 ng·m⁻³, respectively. And the concentrations of six metals over the BS and
414 the YS markedly surpassed those recorded in other seas, and were 6-60 times higher than the concentrations over the NWP. In
415 contrast, the deposition fluxes of the six metals varied much less over different sea areas, and can affect more remote waters,



416 such as the NWP. Pollutants carried by dust, especially Fe and Al, were transported to more open sea areas through intense
417 weather processes. The spatial distribution of deposition flux for these two metals in the sea areas was broader than that of the
418 remaining four metals. The annual soluble deposition fluxes of Fe, Al, V, Ni, Zn, and Cu were 646.8, 1799.6, 43.3, 36.3, 118.4,
419 and 42.9 $\mu\text{g}\cdot\text{m}^{-2}$, respectively. The contribution of land anthropogenic sources to fine-mode soluble iron was significant (>94%
420 across all sea areas), and dust sources contributed a lot to coarse-mode soluble iron (ranged from 29% to 85%). Particulate
421 matter emitted by anthropogenic sources is more acidic than that from dust sources and is distributed in a higher percentage in
422 the fine mode, allowing for longer particle aging processes. As a result, higher soluble iron deposition fluxes in the fine mode
423 compared to the coarse mode.

424 Both land-based and marine-based anthropogenic sources (as known as shipping) played more important roles on maritime
425 deposition flux compared to emissions. But the impact of dust on depositional fluxes was not as large as its impact on emissions
426 for East Asian seas. Land anthropogenic sources dominated or co-dominated the deposition of most metals and soluble iron in
427 East Asian seas. Ship sources dominated the deposition of V and Ni in most of the sea areas. Only the soluble iron deposition
428 in Spring was dust-dominated, which is associated with the seasonal characteristics of Asian dust, mostly occurring in spring.

429 This study provides gridded data on atmospheric deposition fluxes with detailed source categories, and identifies the
430 dominant source of metal deposition in the ocean for future assessments of the impact of trace metals on marine ecology. It
431 offers a comprehensive analysis of contributions from various sources, establishing the groundwork for a more profound
432 understanding of the contributions of human activities and natural processes to metal distribution in marine areas. However,
433 further research is still needed in the future to investigate the concentrations, deposition, and solubility of metal elements in
434 marine environments, aiming to enhance the accuracy of estimates for soluble metal deposition flux.

435 **Author contribution**

436 Shenglan Jiang: Writing - original draft preparation, Investigation, Methodology, Software, Validation, Formal analysis, Data
437 curation, Visualization.

438 Yan Zhang: Conceptualization, Investigation, Supervision, Methodology, Validation, Formal analysis, Writing - review &
439 editing, Project administration, Funding acquisition.

440 Guangyuan Yu: Validation, Investigation, Writing review & editing.

441 Zimin Han: Data curation, Software.

442 Junri Zhao: Data curation, Investigation, Methodology.

443 Tianle Zhang: Data curation, Writing - review & editing.

444 Mei Zheng: Writing – review, Funding acquisition.



445 **Code/Data availability**

446 The Final Analysis (FNL) meteorological data from are available from National Centres for Environmental Predictions (NCEP)
447 at <https://rda.ucar.edu/datasets/ds083.2>. The base source code of CMAQv5.4 is available at <https://github.com/USEPA/CMAQ>.
448 The model data presented in this paper can be obtained from Yan Zhang (yan_zhang@fudan.edu.cn) upon request.

449 **Competing interests**

450 The authors declare that they have no conflict of interest.

451 **Acknowledgements**

452 The work was supported by the National Natural Science Foundation of China (No. 42375100, No. 42030708), the Natural
453 Science Foundation of Shanghai Committee of Science and Technology, China (No. 22ZR1407700), and the Program of
454 Pudong Committee of Science and Technology, Shanghai (No. PKJ2022-C05).

455 **References**

- 456 Alexander, B., Park, R. J., Jacob, D. J., and Gong, S.: Transition metal-catalyzed oxidation of atmospheric sulfur: Global
457 implications for the sulfur budget, *Journal of Geophysical Research: Atmospheres*, 114, 10.1029/2008JD010486, 2009.
- 458 Amedro, D., Berasategui, M., Bunkan, A. J. C., Pozzer, A., Lelieveld, J., and Crowley, J. N.: Kinetics of the
459 OH+NO₂ reaction: effect of water vapour and new parameterization for global modelling, *Atmos. Chem.*
460 *Phys.*, 20, 3091-3105, 10.5194/acp-20-3091-2020, 2020.
- 461 Bai, X., Luo, L., Tian, H., Liu, S., Hao, Y., Zhao, S., Lin, S., Zhu, C., Guo, Z., and Lv, Y.: Atmospheric Vanadium Emission
462 Inventory from Both Anthropogenic and Natural Sources in China, *Environmental Science & Technology*, 55, 11568-
463 11578, 10.1021/acs.est.1c04766, 2021.
- 464 Baker, A. R. and Jickells, T. D.: Atmospheric deposition of soluble trace elements along the Atlantic Meridional Transect
465 (AMT), *Progress in Oceanography*, 158, 41-51, 10.1016/j.pocean.2016.10.002, 2017.
- 466 Baker, A. R., Li, M., and Chance, R.: Trace Metal Fractional Solubility in Size-Segregated Aerosols From the Tropical Eastern
467 Atlantic Ocean, *Global Biogeochemical Cycles*, 34, e2019GB006510, 10.1029/2019GB006510, 2020.
- 468 Baker, A. R., Kanakidou, M., Nenes, A., Myriokefalitakis, S., Croot, P. L., Duce, R. A., Gao, Y., Guieu, C., Ito, A., Jickells,
469 T. D., Mahowald, N. M., Middag, R., Perron, M. M. G., Sarin, M. M., Shelley, R., and Turner, D. R.: Changing
470 atmospheric acidity as a modulator of nutrient deposition and ocean biogeochemistry, *Science Advances*, 7, eabd8800,
471 doi:10.1126/sciadv.abd8800, 2021.



- 472 Barkley, A. E., Prospero, J. M., Mahowald, N., Hamilton, D. S., Popendorf, K. J., Oehlert, A. M., Pourmand, A., Gatineau, A.,
473 Panechou-Pulcherie, K., Blackwelder, P., and Gaston, C. J.: African biomass burning is a substantial source of phosphorus
474 deposition to the Amazon, Tropical Atlantic Ocean, and Southern Ocean, *Proceedings of the National Academy of*
475 *Sciences*, 116, 16216-16221, 10.1073/pnas.1906091116, 2019.
- 476 Birmili, W., Allen, A. G., Bary, F., and Harrison, R. M.: Trace Metal Concentrations and Water Solubility in Size-Fractionated
477 Atmospheric Particles and Influence of Road Traffic, *Environmental Science & Technology*, 40, 1144-1153,
478 10.1021/es0486925, 2006.
- 479 Böke, H., Göktürk, E. H., Caner-Saltık, E. N., and Demirci, Ş.: Effect of airborne particle on SO₂-calcite reaction, *Applied*
480 *Surface Science*, 140, 70-82, 10.1016/S0169-4332(98)00468-1, 1999.
- 481 Bonnet, S., Guieu, C., Bruyant, F., Prášil, O., Van Wambeke, F., Raimbault, P., Moutin, T., Grob, C., Gorbunov, M. Y., Zehr,
482 J. P., Masquelier, S. M., Garczarek, L., and Claustre, H.: Nutrient limitation of primary productivity in the Southeast
483 Pacific (BIOSOPE cruise), *Biogeosciences*, 5, 215-225, 10.5194/bg-5-215-2008, 2008.
- 484 Bowie, A. R., Lannuzel, D., Remenyi, T. A., Wagener, T., Lam, P. J., Boyd, P. W., Guieu, C., Townsend, A. T., and Trull, T.
485 W.: Biogeochemical iron budgets of the Southern Ocean south of Australia: Decoupling of iron and nutrient cycles in the
486 subantarctic zone by the summertime supply, *Global Biogeochemical Cycles*, 23, 10.1029/2009GB003500, 2009.
- 487 Bray, C. D., Strum, M., Simon, H., Riddick, L., Kosusko, M., Menetrez, M., Hays, M. D., and Rao, V.: An assessment of
488 important SPECIATE profiles in the EPA emissions modeling platform and current data gaps, *Atmospheric Environment*,
489 207, 93-104, 10.1016/j.atmosenv.2019.03.013, 2019.
- 490 Browning, T. J., Achterberg, E. P., Yong, J. C., Rapp, I., Utermann, C., Engel, A., and Moore, C. M.: Iron limitation of
491 microbial phosphorus acquisition in the tropical North Atlantic, *Nature Communications*, 8, 15465,
492 10.1038/ncomms15465, 2017.
- 493 Butler, A.: Acquisition and Utilization of Transition Metal Ions by Marine Organisms, *Science*, 281, 207-209,
494 10.1126/science.281.5374.207, 1998.
- 495 Celo, V., Dabek-Zlotorzynska, E., and McCurdy, M.: Chemical Characterization of Exhaust Emissions from Selected
496 Canadian Marine Vessels: The Case of Trace Metals and Lanthanoids, *Environmental Science & Technology*, 49, 5220-
497 5226, 10.1021/acs.est.5b00127, 2015.
- 498 Chen, D., Wang, X., Li, Y., Lang, J., Zhou, Y., Guo, X., and Zhao, Y.: High-spatiotemporal-resolution ship emission inventory
499 of China based on AIS data in 2014, *Science of The Total Environment*, 609, 776-787, 10.1016/j.scitotenv.2017.07.051,
500 2017.
- 501 Chen, H., Laskin, A., Baltusaitis, J., Gorski, C. A., Scherer, M. M., and Grassian, V. H.: Coal Fly Ash as a Source of Iron in
502 Atmospheric Dust, *Environmental Science & Technology*, 46, 2112-2120, 10.1021/es204102f, 2012.
- 503 Cheng, I., Mamun, A. A., and Zhang, L.: A synthesis review on atmospheric wet deposition of particulate elements: scavenging
504 ratios, solubility, and flux measurements, *Environmental Reviews*, 29, 340-353, 10.1139/er-2020-0118, 2021.



- 505 Chester, R., Murphy, K. J. T., Lin, F. J., Berry, A. S., Bradshaw, G. A., and Corcoran, P. A.: Factors controlling the solubilities
506 of trace metals from non-remote aerosols deposited to the sea surface by the ‘dry’ deposition mode, *Marine Chemistry*,
507 42, 107-126, 10.1016/0304-4203(93)90241-F, 1993.
- 508 Connan, O., Maro, D., Hébert, D., Roupsard, P., Goujon, R., Letellier, B., and Le Cavalier, S.: Wet and dry deposition of
509 particles associated metals (Cd, Pb, Zn, Ni, Hg) in a rural wetland site, Marais Vernier, France, *Atmospheric Environment*,
510 67, 394-403, 10.1016/j.atmosenv.2012.11.029, 2013.
- 511 Corbin, J. C., Mensah, A. A., Pieber, S. M., Orasche, J., Michalke, B., Zanatta, M., Czech, H., Massabò, D., Buatier de Mongeot,
512 F., Mennucci, C., El Haddad, I., Kumar, N. K., Stengel, B., Huang, Y., Zimmermann, R., Prévôt, A. S. H., and Gysel, M.:
513 Trace Metals in Soot and PM_{2.5} from Heavy-Fuel-Oil Combustion in a Marine Engine, *Environmental Science &*
514 *Technology*, 52, 6714-6722, 10.1021/acs.est.8b01764, 2018.
- 515 Crippa, M., Solazzo, E., Huang, G., Guizzardi, D., Koffi, E., Muntean, M., Schieberle, C., Friedrich, R., and Janssens-
516 Maenhout, G.: High resolution temporal profiles in the Emissions Database for Global Atmospheric Research, *Scientific*
517 *Data*, 7, 121, 10.1038/s41597-020-0462-2, 2020.
- 518 de Baar, H. J. W., van Heuven, S. M. A. C., and Middag, R.: Ocean Biochemical Cycling and Trace Elements, in: *Encyclopedia*
519 *of Geochemistry: A Comprehensive Reference Source on the Chemistry of the Earth*, edited by: White, W. M., Springer
520 International Publishing, Cham, 1023-1042, 10.1007/978-3-319-39312-4_356, 2018.
- 521 Fan, Q., Zhang, Y., Ma, W., Ma, H., Feng, J., Yu, Q., Yang, X., Ng, S. K. W., Fu, Q., and Chen, L.: Spatial and Seasonal
522 Dynamics of Ship Emissions over the Yangtze River Delta and East China Sea and Their Potential Environmental
523 Influence, *Environmental Science & Technology*, 50, 1322-1329, 10.1021/acs.est.5b03965, 2016.
- 524 Fu, Y., Tang, Y., Shu, X., Hopke, P. K., He, L., Ying, Q., Xia, Z., Lei, M., and Qiao, X.: Changes of atmospheric metal(loid)
525 deposition from 2017 to 2021 at Mount Emei under China's air pollution control strategy, *Atmospheric Environment*, 302,
526 119714, 10.1016/j.atmosenv.2023.119714, 2023.
- 527 Gao, Y., Xu, G., Zhan, J., Zhang, J., Li, W., Lin, Q., Chen, L., and Lin, H.: Spatial and particle size distributions of atmospheric
528 dissolvable iron in aerosols and its input to the Southern Ocean and coastal East Antarctica, *Journal of Geophysical*
529 *Research: Atmospheres*, 118, 12,634-612,648, 10.1002/2013JD020367, 2013.
- 530 Gargava, P., Chow, J. C., Watson, J. G., and Lowenthal, D. H.: Speciated PM₁₀ Emission Inventory for Delhi, India, *Aerosol*
531 *and Air Quality Research*, 14, 1515-1526, 10.4209/aaqr.2013.02.0047, 2014.
- 532 Gui, K., Yao, W., Che, H., An, L., Zheng, Y., Li, L., Zhao, H., Zhang, L., Zhong, J., Wang, Y., and Zhang, X.: Record-breaking
533 dust loading during two mega dust storm events over northern China in March 2021: aerosol optical and radiative
534 properties and meteorological drivers, *Atmos. Chem. Phys.*, 22, 7905-7932, 10.5194/acp-22-7905-2022, 2022.
- 535 Guo, J., Lapi, S., Ruth, T. J., and Maldonado, M. T.: THE EFFECTS OF IRON AND COPPER AVAILABILITY ON THE
536 COPPER STOICHIOMETRY OF MARINE PHYTOPLANKTON1, *Journal of Phycology*, 48, 312-325, 10.1111/j.1529-
537 8817.2012.01133.x, 2012.



- 538 Hamilton, D. S., Baker, A. R., Iwamoto, Y., Gassó, S., Bergas-Masso, E., Deutch, S., Dinasquet, J., Kondo, Y., Llort, J.,
539 Myriokefalitakis, S., Perron, M. M. G., Wegmann, A., and Yoon, J.-E.: An aerosol odyssey: Navigating nutrient flux
540 changes to marine ecosystems, *Elementa: Science of the Anthropocene*, 11, 10.1525/elementa.2023.00037, 2023.
- 541 Hamilton, D. S., Perron, M. M. G., Bond, T. C., Bowie, A. R., Buchholz, R. R., Guieu, C., Ito, A., Maenhaut, W.,
542 Myriokefalitakis, S., Olgun, N., Rathod, S. D., Schepanski, K., Tagliabue, A., Wagner, R., and Mahowald, N. M.: Earth,
543 Wind, Fire, and Pollution: Aerosol Nutrient Sources and Impacts on Ocean Biogeochemistry, *Annual Review of Marine
544 Science*, 14, 303-330, 10.1146/annurev-marine-031921-013612, 2022.
- 545 Hsu, S.-C., Wong, G. T. F., Gong, G.-C., Shiah, F.-K., Huang, Y.-T., Kao, S.-J., Tsai, F., Candice Lung, S.-C., Lin, F.-J., Lin,
546 I. I., Hung, C.-C., and Tseng, C.-M.: Sources, solubility, and dry deposition of aerosol trace elements over the East China
547 Sea, *Marine Chemistry*, 120, 116-127, 10.1016/j.marchem.2008.10.003, 2010.
- 548 Ito, A.: Atmospheric Processing of Combustion Aerosols as a Source of Bioavailable Iron, *Environmental Science &
549 Technology Letters*, 2, 70-75, 10.1021/acs.estlett.5b00007, 2015.
- 550 Ito, A., Ye, Y., Baldo, C., and Shi, Z.: Ocean fertilization by pyrogenic aerosol iron, *npj Climate and Atmospheric Science*, 4,
551 30, 10.1038/s41612-021-00185-8, 2021.
- 552 Ito, A., Myriokefalitakis, S., Kanakidou, M., Mahowald, N. M., Scanza, R. A., Hamilton, D. S., Baker, A. R., Jickells, T.,
553 Sarin, M., Bikkina, S., Gao, Y., Shelley, R. U., Buck, C. S., Landing, W. M., Bowie, A. R., Perron, M. M. G., Guieu, C.,
554 Meskhidze, N., Johnson, M. S., Feng, Y., Kok, J. F., Nenes, A., and Duce, R. A.: Pyrogenic iron: The missing link to
555 high iron solubility in aerosols, *Science Advances*, 5, eaau7671, 10.1126/sciadv.aau7671, 2019.
- 556 Kajino, M., Hagino, H., Fujitani, Y., Morikawa, T., Fukui, T., Onishi, K., Okuda, T., Kajikawa, T., and Igarashi, Y.: Modeling
557 Transition Metals in East Asia and Japan and Its Emission Sources, *GeoHealth*, 4, e2020GH000259,
558 10.1029/2020GH000259, 2020.
- 559 Kurisu, M., Sakata, K., Uematsu, M., Ito, A., and Takahashi, Y.: Contribution of combustion Fe in marine aerosols over the
560 northwestern Pacific estimated by Fe stable isotope ratios, *Atmos. Chem. Phys.*, 21, 16027-16050, 10.5194/acp-21-
561 16027-2021, 2021.
- 562 Lana, A., Bell, T. G., Simó, R., Vallina, S. M., Ballabrera-Poy, J., Kettle, A. J., Dachs, J., Bopp, L., Saltzman, E. S., Stefels,
563 J., Johnson, J. E., and Liss, P. S.: An updated climatology of surface dimethylsulfide concentrations and emission fluxes
564 in the global ocean, *Global Biogeochemical Cycles*, 25, 10.1029/2010GB003850, 2011.
- 565 Li, J. and Chen, S.-H.: Dust impacts on Mongolian cyclone and cold front in East Asia: a case study during 18–22 March 2010,
566 *Frontiers in Environmental Science*, 11, 10.3389/fenvs.2023.1167232, 2023.
- 567 Li, W., Xu, L., Liu, X., Zhang, J., Lin, Y., Yao, X., Gao, H., Zhang, D., Chen, J., Wang, W., Harrison, R. M., Zhang, X., Shao,
568 L., Fu, P., Nenes, A., and Shi, Z.: Air pollution–aerosol interactions produce more bioavailable iron for ocean ecosystems,
569 *Science Advances*, 3, e1601749, 10.1126/sciadv.1601749, 2017.



- 570 Little, S. H., Vance, D., Walker-Brown, C., and Landing, W. M.: The oceanic mass balance of copper and zinc isotopes,
571 investigated by analysis of their inputs, and outputs to ferromanganese oxide sediments, *Geochimica et Cosmochimica*
572 *Acta*, 125, 673-693, 10.1016/j.gca.2013.07.046, 2014.
- 573 Liu, M., Matsui, H., Hamilton, D. S., Lamb, K. D., Rathod, S. D., Schwarz, J. P., and Mahowald, N. M.: The underappreciated
574 role of anthropogenic sources in atmospheric soluble iron flux to the Southern Ocean, *npj Climate and Atmospheric*
575 *Science*, 5, 28, 10.1038/s41612-022-00250-w, 2022.
- 576 Longhini, C. M., Sá, F., and Neto, R. R.: Review and synthesis: iron input, biogeochemistry, and ecological approaches in
577 seawater, *Environmental Reviews*, 27, 125-137, 10.1139/er-2018-0020, 2019.
- 578 Mackey, K. R. M., Post, A. F., McIlvin, M. R., Cutter, G. A., John, S. G., and Saito, M. A.: Divergent responses of Atlantic
579 coastal and oceanic *Synechococcus* to iron limitation, *Proceedings of the National Academy of Sciences*, 112,
580 9944-9949, 10.1073/pnas.1509448112, 2015.
- 581 Mahowald, N. M., Hamilton, D. S., Mackey, K. R. M., Moore, J. K., Baker, A. R., Scanza, R. A., and Zhang, Y.: Aerosol trace
582 metal leaching and impacts on marine microorganisms, *Nature Communications*, 9, 2614, 10.1038/s41467-018-04970-7,
583 2018.
- 584 Mahowald, N. M., Baker, A. R., Bergametti, G., Brooks, N., Duce, R. A., Jickells, T. D., Kubilay, N., Prospero, J. M., and
585 Tegen, I.: Atmospheric global dust cycle and iron inputs to the ocean, *Global Biogeochemical Cycles*, 19,
586 10.1029/2004GB002402, 2005.
- 587 Mahowald, N. M., Engelstaedter, S., Luo, C., Sealy, A., Artaxo, P., Benitez-Nelson, C., Bonnet, S., Chen, Y., Chuang, P. Y.,
588 Cohen, D. D., Dulac, F., Herut, B., Johansen, A. M., Kubilay, N., Losno, R., Maenhaut, W., Paytan, A., Prospero, J. M.,
589 Shank, L. M., and Siefert, R. L.: Atmospheric Iron Deposition: Global Distribution, Variability, and Human Perturbations,
590 *Annual Review of Marine Science*, 1, 245-278, 10.1146/annurev.marine.010908.163727, 2009.
- 591 Mahowald, N. M., Kloster, S., Engelstaedter, S., Moore, J. K., Mukhopadhyay, S., McConnell, J. R., Albani, S., Doney, S. C.,
592 Bhattacharya, A., Curran, M. A. J., Flanner, M. G., Hoffman, F. M., Lawrence, D. M., Lindsay, K., Mayewski, P. A.,
593 Neff, J., Rothenberg, D., Thomas, E., Thornton, P. E., and Zender, C. S.: Observed 20th century desert dust variability:
594 impact on climate and biogeochemistry, *Atmos. Chem. Phys.*, 10, 10875-10893, 10.5194/acp-10-10875-2010, 2010.
- 595 Matsui, H., Mahowald, N. M., Moteki, N., Hamilton, D. S., Ohata, S., Yoshida, A., Koike, M., Scanza, R. A., and Flanner, M.
596 G.: Anthropogenic combustion iron as a complex climate forcer, *Nature Communications*, 9, 1593, 10.1038/s41467-018-
597 03997-0, 2018.
- 598 Morel, F. M. M. and Price, N. M.: The Biogeochemical Cycles of Trace Metals in the Oceans, *Science*, 300, 944-947,
599 10.1126/science.1083545, 2003.
- 600 Morel, F. M. M., Reinfelder, J. R., Roberts, S. B., Chamberlain, C. P., Lee, J. G., and Yee, D.: Zinc and carbon co-limitation
601 of marine phytoplankton, *Nature*, 369, 740-742, 10.1038/369740a0, 1994.
- 602 Nuester, J., Vogt, S., Newville, M., Kustka, A., and Twining, B.: The Unique Biogeochemical Signature of the Marine
603 Diazotroph *Trichodesmium*, *Frontiers in Microbiology*, 3, 10.3389/fmicb.2012.00150, 2012.



- 604 Oakes, M., Ingall, E. D., Lai, B., Shafer, M. M., Hays, M. D., Liu, Z. G., Russell, A. G., and Weber, R. J.: Iron Solubility
605 Related to Particle Sulfur Content in Source Emission and Ambient Fine Particles, *Environmental Science & Technology*,
606 46, 6637-6644, 10.1021/es300701c, 2012.
- 607 Okubo, A., Takeda, S., and Obata, H.: Atmospheric deposition of trace metals to the western North Pacific Ocean observed at
608 coastal station in Japan, *Atmospheric Research*, 129-130, 20-32, 10.1016/j.atmosres.2013.03.014, 2013.
- 609 Pan, Y., Liu, J., Zhang, L., Cao, J., Hu, J., Tian, S., Li, X., and Xu, W.: Bulk Deposition and Source Apportionment of
610 Atmospheric Heavy Metals and Metalloids in Agricultural Areas of Rural Beijing during 2016–2020, *Atmosphere*, 12,
611 283, 10.3390/atmos12020283, 2021.
- 612 Pan, Y. P. and Wang, Y. S.: Atmospheric wet and dry deposition of trace elements at 10 sites in Northern China, *Atmos. Chem.*
613 *Phys.*, 15, 951-972, 10.5194/acp-15-951-2015, 2015.
- 614 Reff, A., Bhave, P. V., Simon, H., Pace, T. G., Pouliot, G. A., Mobley, J. D., and Houyoux, M.: Emissions Inventory of PM_{2.5}
615 Trace Elements across the United States, *Environmental Science & Technology*, 43, 5790-5796, 10.1021/es802930x,
616 2009.
- 617 Rodriguez, I. B. and Ho, T.-Y.: Diel nitrogen fixation pattern of *Trichodesmium*: the interactive control of light and Ni,
618 *Scientific Reports*, 4, 4445, 10.1038/srep04445, 2014.
- 619 Sakata, M. and Asakura, K.: Atmospheric dry deposition of trace elements at a site on Asian-continent side of Japan,
620 *Atmospheric Environment*, 45, 1075-1083, 10.1016/j.atmosenv.2010.11.043, 2011.
- 621 Sarwar, G., Gantt, B., Foley, K., Fahey, K., Spero, T. L., Kang, D., Mathur, R., Foroutan, H., Xing, J., Sherwen, T., and Saiz-
622 Lopez, A.: Influence of bromine and iodine chemistry on annual, seasonal, diurnal, and background ozone: CMAQ
623 simulations over the Northern Hemisphere, *Atmospheric Environment*, 213, 395-404, 10.1016/j.atmosenv.2019.06.020,
624 2019.
- 625 Schmidt, K., Schlosser, C., Atkinson, A., Fielding, S., Venables, Hugh J., Waluda, Claire M., and Achterberg, Eric P.:
626 Zooplankton Gut Passage Mobilizes Lithogenic Iron for Ocean Productivity, *Current Biology*, 26, 2667-2673,
627 10.1016/j.cub.2016.07.058, 2016.
- 628 Shaked, Y., Xu, Y., Leblanc, K., and Morel, F. M. M.: Zinc availability and alkaline phosphatase activity in *Emiliana huxleyi*:
629 Implications for Zn-P co-limitation in the ocean, *Limnology and Oceanography*, 51, 299-309, 10.4319/lo.2006.51.1.0299,
630 2006.
- 631 Shao, J., Chen, Q., Wang, Y., Lu, X., He, P., Sun, Y., Shah, V., Martin, R. V., Philip, S., Song, S., Zhao, Y., Xie, Z., Zhang,
632 L., and Alexander, B.: Heterogeneous sulfate aerosol formation mechanisms during wintertime Chinese haze events: air
633 quality model assessment using observations of sulfate oxygen isotopes in Beijing, *Atmos. Chem. Phys.*, 19, 6107-6123,
634 10.5194/acp-19-6107-2019, 2019.
- 635 Shi, J.-H., Zhang, J., Gao, H.-W., Tan, S.-C., Yao, X.-H., and Ren, J.-L.: Concentration, solubility and deposition flux of
636 atmospheric particulate nutrients over the Yellow Sea, *Deep Sea Research Part II: Topical Studies in Oceanography*, 97,
637 43-50, 10.1016/j.dsr2.2013.05.004, 2013.



- 638 Shi, Z., Krom, M. D., Bonneville, S., and Benning, L. G.: Atmospheric Processing Outside Clouds Increases Soluble Iron in
639 Mineral Dust, *Environmental Science & Technology*, 49, 1472-1477, 10.1021/es504623x, 2015.
- 640 Shi, Z., Endres, S., Rutgersson, A., Al-Hajjaji, S., Brynolf, S., Booge, D., Hassellöv, I.-M., Kontovas, C., Kumar, R., Liu, H.,
641 Marandino, C., Matthias, V., Moldanová, J., Salo, K., Sebe, M., Yi, W., Yang, M., and Zhang, C.: Perspectives on
642 shipping emissions and their impacts on the surface ocean and lower atmosphere: An environmental-social-economic
643 dimension, *Elementa: Science of the Anthropocene*, 11, 10.1525/elementa.2023.00052, 2023.
- 644 Sholkovitz, E. R., Sedwick, P. N., Church, T. M., Baker, A. R., and Powell, C. F.: Fractional solubility of aerosol iron:
645 Synthesis of a global-scale data set, *Geochimica et Cosmochimica Acta*, 89, 173-189, 10.1016/j.gca.2012.04.022, 2012.
- 646 Simon, H., Beck, L., Bhave, P. V., Divita, F., Hsu, Y., Luecken, D., Mobley, J. D., Pouliot, G. A., Reff, A., Sarwar, G., and
647 Strum, M.: The development and uses of EPA's SPECIATE database, *Atmospheric Pollution Research*, 1, 196-206,
648 10.5094/APR.2010.026, 2010.
- 649 Sunda, W.: Feedback Interactions between Trace Metal Nutrients and Phytoplankton in the Ocean, *Frontiers in Microbiology*,
650 3, 10.3389/fmicb.2012.00204, 2012.
- 651 Takano, S., Tanimizu, M., Hirata, T., and Sohrin, Y.: Isotopic constraints on biogeochemical cycling of copper in the ocean,
652 *Nature Communications*, 5, 5663, 10.1038/ncomms6663, 2014.
- 653 Tao, J., Zhang, L., Zhang, R., Wu, Y., Zhang, Z., Zhang, X., Tang, Y., Cao, J., and Zhang, Y.: Uncertainty assessment of
654 source attribution of PM_{2.5} and its water-soluble organic carbon content using different biomass burning tracers in
655 positive matrix factorization analysis — a case study in Beijing, China, *Science of The Total Environment*, 543, 326-335,
656 10.1016/j.scitotenv.2015.11.057, 2016.
- 657 Tao, J., Zhang, L., Cao, J., Zhong, L., Chen, D., Yang, Y., Chen, D., Chen, L., Zhang, Z., Wu, Y., Xia, Y., Ye, S., and Zhang,
658 R.: Source apportionment of PM_{2.5} at urban and suburban areas of the Pearl River Delta region, south China - With
659 emphasis on ship emissions, *Science of The Total Environment*, 574, 1559-1570, 10.1016/j.scitotenv.2016.08.175, 2017.
- 660 Tian, H. Z., Zhu, C. Y., Gao, J. J., Cheng, K., Hao, J. M., Wang, K., Hua, S. B., Wang, Y., and Zhou, J. R.: Quantitative
661 assessment of atmospheric emissions of toxic heavy metals from anthropogenic sources in China: historical trend, spatial
662 distribution, uncertainties, and control policies, *Atmos. Chem. Phys.*, 15, 10127-10147, 10.5194/acp-15-10127-2015,
663 2015.
- 664 Tortell, P. D., Rau, G. H., and Morel, F. M. M.: Inorganic carbon acquisition in coastal Pacific phytoplankton communities,
665 *Limnology and Oceanography*, 45, 1485-1500, 10.4319/lo.2000.45.7.1485, 2000.
- 666 Us, E. P. A.: CMAQ Model Version 5.3 Input Data -- 1/1/2016 - 12/31/2016 12km CONUS (V1), UNC Dataverse [dataset],
667 doi:10.15139/S3/MHNUNE, 2019.
- 668 Wang, F. J., Chen, Y., Guo, Z. G., Gao, H. W., Mackey, K. R., Yao, X. H., Zhuang, G. S., and Paytan, A.: Combined effects
669 of iron and copper from atmospheric dry deposition on ocean productivity, *Geophysical Research Letters*, 44, 2546-2555,
670 10.1002/2016GL072349, 2017a.



- 671 Wang, K., Tian, H., Hua, S., Zhu, C., Gao, J., Xue, Y., Hao, J., Wang, Y., and Zhou, J.: A comprehensive emission inventory
672 of multiple air pollutants from iron and steel industry in China: Temporal trends and spatial variation characteristics,
673 *Science of The Total Environment*, 559, 7-14, 10.1016/j.scitotenv.2016.03.125, 2016.
- 674 Wang, Y., Cheng, K., Wu, W., Tian, H., Yi, P., Zhi, G., Fan, J., and Liu, S.: Atmospheric emissions of typical toxic heavy
675 metals from open burning of municipal solid waste in China, *Atmospheric Environment*, 152, 6-15,
676 10.1016/j.atmosenv.2016.12.017, 2017b.
- 677 Wei, Z., Wang, L. T., Chen, M. Z., and Zheng, Y.: The 2013 severe haze over the Southern Hebei, China: PM_{2.5} composition
678 and source apportionment, *Atmospheric Pollution Research*, 5, 759-768, 10.5094/APR.2014.085, 2014.
- 679 Whitfield, M.: Interactions between phytoplankton and trace metals in the ocean, in: *Advances in Marine Biology*, Academic
680 Press, 1-128, 10.1016/S0065-2881(01)41002-9, 2001.
- 681 Wuttig, K., Heller, M. I., and Croot, P. L.: Reactivity of Inorganic Mn and Mn Desferrioxamine B with O₂, O₂⁻, and H₂O₂
682 in Seawater, *Environmental Science & Technology*, 47, 10257-10265, 10.1021/es4016603, 2013a.
- 683 Wuttig, K., Wagener, T., Bressac, M., Dammshäuser, A., Streu, P., Guieu, C., and Croot, P. L.: Impacts of dust deposition on
684 dissolved trace metal concentrations (Mn, Al and Fe) during a mesocosm experiment, *Biogeosciences*, 10, 2583-2600,
685 10.5194/bg-10-2583-2013, 2013b.
- 686 Xu, L., Pye, H. O. T., He, J., Chen, Y., Murphy, B. N., and Ng, N. L.: Experimental and model estimates of the contributions
687 from biogenic monoterpenes and sesquiterpenes to secondary organic aerosol in the southeastern United States, *Atmos.*
688 *Chem. Phys.*, 18, 12613-12637, 10.5194/acp-18-12613-2018, 2018.
- 689 Xuan, J.: Emission inventory of eight elements, Fe, Al, K, Mg, Mn, Na, Ca and Ti, in dust source region of East Asia,
690 *Atmospheric Environment*, 39, 813-821, 10.1016/j.atmosenv.2004.10.029, 2005.
- 691 Yamamoto, A., Hajima, T., Yamazaki, D., Noguchi Aita, M., Ito, A., and Kawamiya, M.: Competing and accelerating effects
692 of anthropogenic nutrient inputs on climate-driven changes in ocean carbon and oxygen cycles, *Science Advances*, 8,
693 eabl9207, doi:10.1126/sciadv.abl9207, 2022.
- 694 Yang, T., Chen, Y., Zhou, S., and Li, H.: Impacts of Aerosol Copper on Marine Phytoplankton: A Review, *Atmosphere*, 10,
695 414, 10.3390/atmos10070414, 2019.
- 696 Ying, Q., Feng, M., Song, D., Wu, L., Hu, J., Zhang, H., Kleeman, M. J., and Li, X.: Improve regional distribution and source
697 apportionment of PM_{2.5} trace elements in China using inventory-observation constrained emission factors, *Science of*
698 *The Total Environment*, 624, 355-365, 10.1016/j.scitotenv.2017.12.138, 2018.
- 699 Yuan, Y., Zhang, Y., Mao, J., Yu, G., Xu, K., Zhao, J., Qian, H., Wu, L., Yang, X., Chen, Y., and Ma, W.: Diverse changes in
700 shipping emissions around the Western Pacific ports under the coeffect of the epidemic and fuel oil policy, *Science of*
701 *The Total Environment*, 879, 162892, 10.1016/j.scitotenv.2023.162892, 2023.
- 702 Zhai, J., Yu, G., Zhang, J., Shi, S., Yuan, Y., Jiang, S., Xing, C., Cai, B., Zeng, Y., Wang, Y., Zhang, A., Zhang, Y., Fu, T.-
703 M., Zhu, L., Shen, H., Ye, J., Wang, C., Tao, S., Li, M., Zhang, Y., and Yang, X.: Impact of Ship Emissions on Air



704 Quality in the Greater Bay Area in China under the Latest Global Marine Fuel Regulation, *Environmental Science &*
705 *Technology*, 57, 12341-12350, 10.1021/acs.est.3c03950, 2023.

706 Zhang, H., Li, R., Dong, S., Wang, F., Zhu, Y., Meng, H., Huang, C., Ren, Y., Wang, X., Hu, X., Li, T., Peng, C., Zhang, G.,
707 Xue, L., Wang, X., and Tang, M.: Abundance and Fractional Solubility of Aerosol Iron During Winter at a Coastal City
708 in Northern China: Similarities and Contrasts Between Fine and Coarse Particles, *Journal of Geophysical Research:*
709 *Atmospheres*, 127, e2021JD036070, 10.1029/2021JD036070, 2022.

710 Zhang, T., Liu, J., Xiang, Y., Liu, X., Zhang, J., Zhang, L., Ying, Q., Wang, Y., Wang, Y., Chen, S., Chai, F., and Zheng, M.:
711 Quantifying anthropogenic emission of iron in marine aerosol in the Northwest Pacific with shipborne online
712 measurements, *Science of The Total Environment*, 912, 169158, 10.1016/j.scitotenv.2023.169158, 2024.

713 Zhao, J., Zhang, Y., Xu, H., Tao, S., Wang, R., Yu, Q., Chen, Y., Zou, Z., and Ma, W.: Trace Elements From Ocean-Going
714 Vessels in East Asia: Vanadium and Nickel Emissions and Their Impacts on Air Quality, *Journal of Geophysical Research:*
715 *Atmospheres*, 126, e2020JD033984, 10.1029/2020JD033984, 2021a.

716 Zhao, J., Zhang, Y., Patton, A. P., Ma, W., Kan, H., Wu, L., Fung, F., Wang, S., Ding, D., and Walker, K.: Projection of ship
717 emissions and their impact on air quality in 2030 in Yangtze River delta, China, *Environmental Pollution*, 263, 114643,
718 10.1016/j.envpol.2020.114643, 2020.

719 Zhao, J., Sarwar, G., Gantt, B., Foley, K., Henderson, B. H., Pye, H. O. T., Fahey, K. M., Kang, D., Mathur, R., Zhang, Y., Li,
720 Q., and Saiz-Lopez, A.: Impact of dimethylsulfide chemistry on air quality over the Northern Hemisphere, *Atmospheric*
721 *Environment*, 244, 117961, 10.1016/j.atmosenv.2020.117961, 2021b.

722 Zou, H.-X., Pang, Q.-Y., Zhang, A.-Q., Lin, L.-D., Li, N., and Yan, X.-F.: Excess copper induced proteomic changes in the
723 marine brown algae *Sargassum fusiforme*, *Ecotoxicology and Environmental Safety*, 111, 271-280,
724 10.1016/j.ecoenv.2014.10.028, 2015.

725